

Downstream Interaction of Lean Premixed Flames

Zhongxian Cheng*, Joseph A. Wehrmeyer, and Robert W. Pitz
Mechanical Engineering Department, Vanderbilt University
Box 1592 Station B, Nashville, TN 37235

Lean premixed combustion has potential advantages of reducing pollutants and improving fuel economy. In some lean engine concepts, the fuel is directly injected into the combustion chamber resulting in a distribution of lean fuel/air mixtures. In this case, very lean mixtures can burn when supported by hot products from more strongly burning flames. This study examines the downstream interaction of opposed jets of a lean-limit hydrocarbon-air mixture vs. a lean hydrogen-air flame. The hydrocarbon (either methane or propane) mixtures are near or below the lean limit. The flame composition is measured by laser-induced Raman scattering and is compared to numerical simulations with detailed chemistry and molecular transport including the thermal-diffusion effect. Several sublimit lean methane-air flames supported by the products from the lean hydrogen-air flame were studied and a small amount of CO₂ product (~1% mole fraction) is formed when the weak methane-air mixture diffuses across the stagnation plane into the hot products from the hydrogen-air flame. Raman scattering measurements and detailed simulations using the four different chemical kinetic mechanisms (GRI 3.0, C1, C2 and Williams) are in excellent agreement. This is converse to earlier measurements in sublimit propane-air flames where CO₂ product measurements were much larger than predictions. Stronger self-propagating methane-air mixtures result in a much higher concentration of product (~6% CO₂ mole fraction) and the simulation results are sensitive to the specific chemical mechanism. These model-data comparisons improve when using either the C2 or the Williams mechanisms. For a series of lean premixed propane flames at various global strain rates, the M5 mechanism and an optimized propane mechanism are used for numerical simulation and show that optimized propane mechanism is reliable for lean propane combustion.

INTRODUCTION

Lean premixed combustion is currently under investigation due to its potential advantages in limiting carbon dioxide, thermal NO_x and reducing fuel consumption. It has been used in gas turbines and direct injection spark ignition (DISI) engines. But a critical problem is that lean combustion tends to produce unburned hydrocarbon pollutants. For example, in DISI engines, ultra-lean combustion is achieved by a stratified charge. The fuel is directly injected into the center of the cylinder late in the compression stroke just prior to the spark. The fuel/air mixture is non-homogeneous, leading to the simultaneous formation of stoichiometric, rich and lean flames inside the cylinder. Lean mixtures can burn when supported by hot products from a more strongly burning flames, thus reducing the formation of unburned hydrocarbons. This interaction of hot products and very lean mixtures is the focus of this work.

The flame occurring in a non-homogeneous region is a typical example of partially premixed flame combustion because reactants are neither completely mixed nor completely separated before combustion [1]. Partially premixed flames have already been studied widely. In particular, downstream interactions between two premixed streams was investigated by Sohrab et al. [2].

Some lean mixtures, normally beyond the flammability limit, become combustible by downstream interaction of the hot product stream with the lean fuel. Sublimit combustion has been discussed for stretched planar [3] and tubular flames [4].

The opposed jet burner generates ideal counterflow flames that are widely used to study chemical kinetics and species transport under aerodynamic stretch. Using opposed jet flames, partially premixed methane-air versus air flame structure was investigated [5]. Lean partially premixed methane and propane flame structures versus hot products have also been investigated [6,7]. In those investigations, major species (reactants and products) concentration and temperature were determined experimentally and compared to numerical predictions.

The present study seeks to extend previous work to a wide range of equivalence ratios and stretch rates. Stretch effects on flame structure and downstream interaction between hot products and lean hydrocarbon mixture are studied. These partially premixed flames are modeled as existing between two opposed jets as shown in Figure 1. The experimental results are compared to numerical predictions obtained from the "Oppdif" part of the CHEMKIN Collection [8]. The global axial strain rate κ of counterflow flames is given by the following equation [9]:

* Corresponding author: zhongxian.cheng@vanderbilt.edu

Associated Web site: <http://www.vuse.vanderbilt.edu/~combust/group.htm>

Proceeding of the Third Joint Meeting of the U.S. Sections of The Combustion Institute

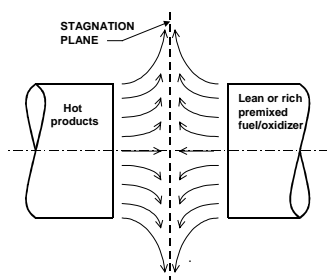


Figure 1. Opposed jet flame schematic.

$$k = \frac{2V_o}{L} \left(1 + \frac{V_F \sqrt{\rho_F}}{V_o \sqrt{\rho_o}} \right)$$

where V is the jet exit velocity, ρ is the gas density, L is the jet separation and subscripts F and O denote the two jets, respectively.

EXPERIMENTS

Measurements of major species and temperature are made along the centerline of an opposed jet burner using a nonintrusive laser diagnostic system. A schematic of the visible Raman system is shown in Figure 2. A detailed description is given earlier [7]. For the present work the opposed jet burner has been modified by inserting honeycomb metal “flow straighteners” into both nozzles. These inserts have 1/32-inch honeycomb cells that are 1/2 inch in length. The inserts provide a very uniform exit velocity profile for both nozzles, as verified by hot wire anemometry traverses in nonreacting flow. In addition the new honeycomb metal inserts do not cause flame attachment of either hydrogen-air or hydrocarbon-air flames. The opposed jet burner was designed by Seshadri et al. [10] and has been used extensively for hydrogen- and hydrocarbon-fueled diffusion flames and for hydrocarbon-fueled premixed flames, but now with the inserts can be used also for lean hydrogen-air premixed flames.

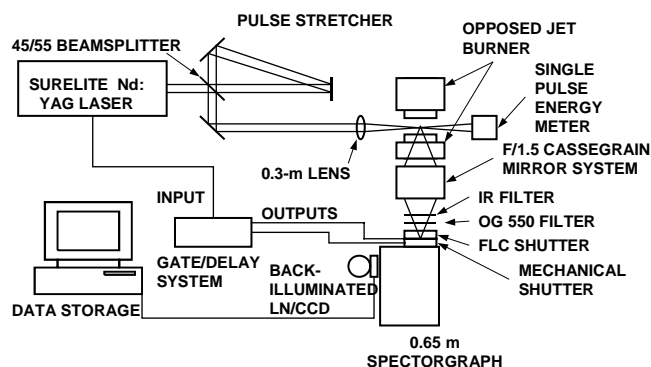


Figure 2. Laser-induced Raman scattering schematic.

FLAMES EXAMINED

Opposed methane and propane-fueled flames are both studied. Each of them has a jet of lean hydrogen-air premixed reactants impinging upon them. Propane is chosen because propane is a relatively simple hydrocarbon fuel, and its chemical burning characteristics more closely represent real fuels, such as gasoline. Methane fuel is another good alternate because of its well-known kinetics. Similar work has already been performed for planar propane-air flames versus hot products [6] and methane-air flames vs. hot products [7], but problems were encountered with the opposed jet burner used at the time [6]. Because premixed hydrogen-air has a fast burning velocity and tends to attach to the mesh screen or sintered metal plate at the nozzle exit (used to provide a top hat velocity profile), the boundary conditions are not well established. A lean hydrogen-air flame is used to generate hot products so that only high temperature water vapor, oxygen and nitrogen impinge upon the hydrocarbon flame. Thus any CO_2 formed must come from the downstream interaction of the hydrocarbon fuel and the hot products.

REACTION MECHANISMS

Detailed chemical kinetic mechanisms and transport data are used for numerical predictions. Four different chemical kinetic mechanisms are used for methane flames: one which models hydrocarbons with only one carbon atom (C_1) [11], one which models hydrocarbons containing up to two carbon atoms (C_2) [11], GRI-Mech 3.0 [12], and Williams et al. [13]. A mechanism called the M5 propane mechanism by Haworth et al. [14] and an optimized reaction model of C_1 - C_3 combustion mechanism by Qin et al. [15] were used for the numerical simulation of propane-air flames.

RESULTS AND DISCUSSION

(1) CH_4 flame versus hot products

Experimental measurements and numerical predictions of temperature and reactant concentrations are compared in Fig. 3 for the $\phi=0.68$ methane-air jet. As seen from the experimental data, a premixed “positive flame speed” flame exists on the side of the stagnation plane for the methane-air mixture. Numerical data is obtained using four different chemical mechanisms. It is found that experimental profiles of all the major species and temperature match very well to the numerically predicted profiles, although the C_1 mechanism does seem to predict a weaker flame than actually exists. The agreement among predictions and experiment is very good for the remaining three mechanisms, taking into consideration experimental uncertainty.

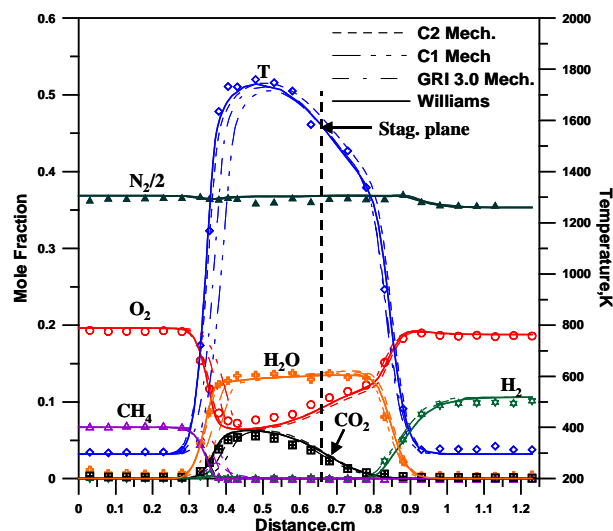


Figure 3. Experimental and numerically-predicted species and temperature profiles for a partially-premixed opposed jet flame: CH₄-air ($\phi=0.68$) vs. H₂-air ($\phi=0.28$), $\kappa=140\text{ s}^{-1}$.

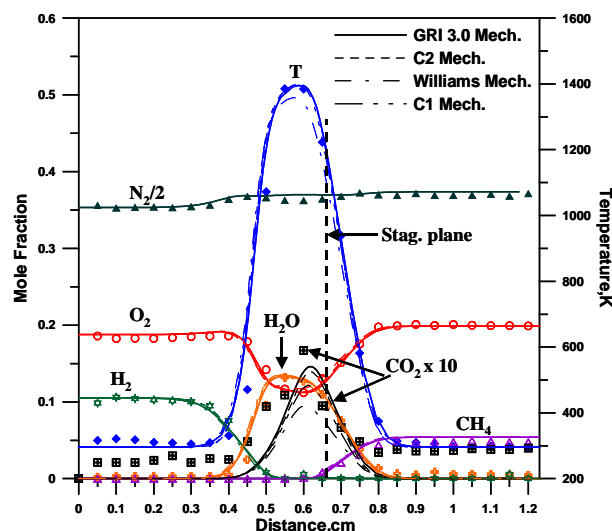


Figure 5. Experimental and numerically-predicted species and temperature profiles for a partially-premixed opposed jet flame: CH₄-air ($\phi=0.54$) vs. H₂-air ($\phi=0.28$), $\kappa=140\text{ s}^{-1}$.

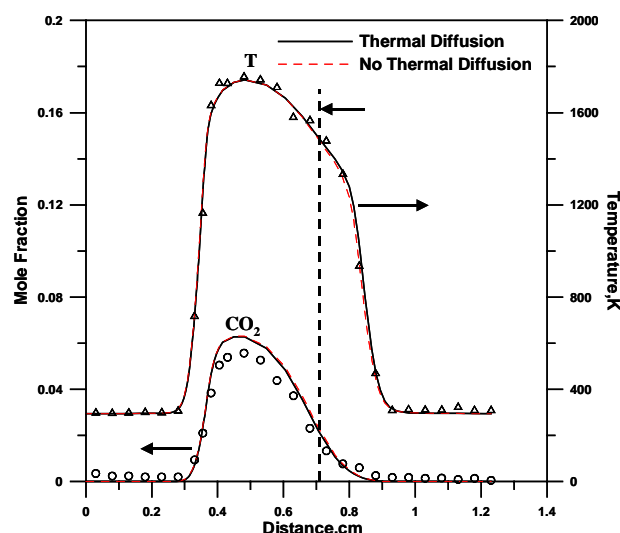


Figure 4. Thermal diffusion effect on flame structure (numerical simulation using Williams mechanism).

Figure 4 shows the effect of thermal diffusion on flame temperature profile and CO₂ concentration profile for the above flame using the Williams mechanism. It is found that there is no significant difference on the methane-air flame side and slight difference on lean hydrogen-air flame side.

Figure 5 shows the experimental results and numerical predictions for a lean methane-air ($\phi=0.54$) mixture impinging upon a hydrogen-air jet ($\phi=0.28$). Here the methane-air mixture is coming from right hand side. There is only a slight difference for this situation compared to the previous “positive flame speed” flame: the methane-air

equivalence ratio is dropped from 0.68 to 0.54. It is found that a lean methane-air premixed “positive flame speed” flame doesn’t exist on the methane-air side of the stagnation plane. Instead a very weak flame is formed by methane diffusing across the stagnation plane and reacting with the excess oxygen from the hydrogen-air premixed flame from the other jet. This weak flame is located at the peak of the CO₂ profile and is called a “negative flame speed” flame [2,16]. The numerically predicted results provided by the four different mechanisms are essentially the same for this negative flame speed flame.

Experimental and numerical results for three negative flame speed flames, each having the same equivalence ratio but different stretch rates, are shown in Figure 6 (The methane-air mixture is on the left hand side). With increasing stretch rate, flame region becomes narrower. Peak temperatures have no significant difference. It appears that stretch doesn’t affect the “negative flame speed” flame too much.

Figure 7 shows flame temperature profiles for a series of flames (ϕ varies from 0.33 to 0.81), which have the same stretch rates ($\kappa=140\text{ s}^{-1}$). The methane-air mixture is on the left hand side. At that stretch rate, sublimit CH₄-air flames ($\phi < 0.5$) and the lean methane-air ($\phi=0.54$) are very weak diffusion flames (negative flame speed flames) and have relatively low flame temperatures (~1300 K).

The downstream flame interaction supports a very weak diffusion flame by supplying either high temperature products (thermal interaction) or radicals (by mass diffusion). Figure 8 shows that the three different downstream hydrogen-air flames (slightly different ϕ) causes significant CO₂ concentration changes. The methane-

air mixture is on the left hand side. Because the premixed hydrogen-air flame has a faster burning velocity when the equivalence ratio increases, this forces the hydrogen-air flame to move toward the jet exit and the two flames to move farther apart. Therefore the diffusion flame is weakened. This is indicated by the lower CO_2 concentration.

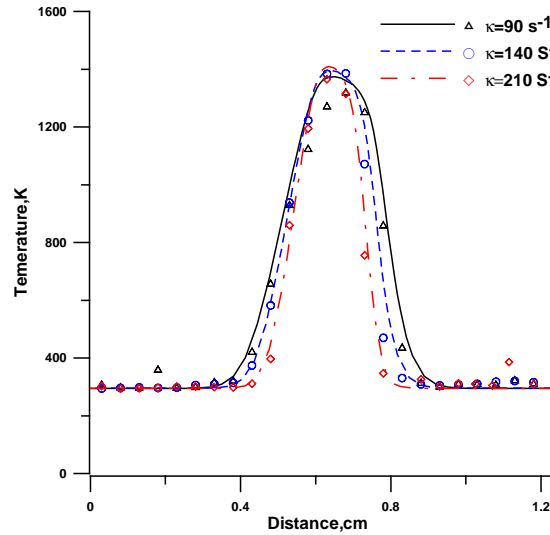


Figure 6. Stretch rate effect on lean diffusion flame structure: CH_4 -air ($\phi=0.54$) vs. H_2 -air ($\phi=0.28$), numerical simulation using GRI 3.0 mechanism.

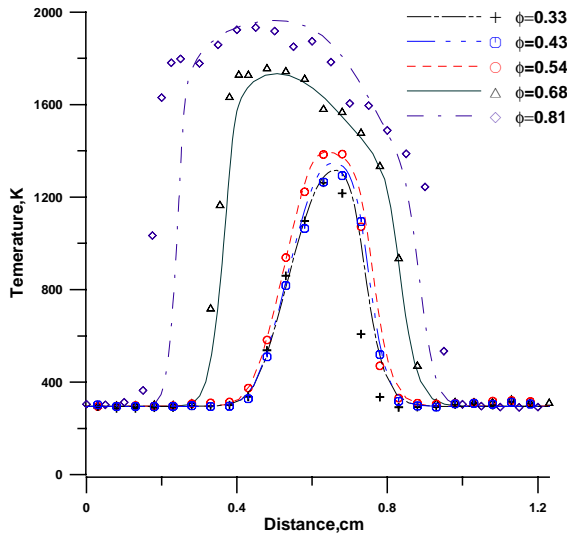


Figure 7. Temperature profiles for partially-premixed opposed jet flames: CH_4 -air ($\phi=0.33\sim 0.81$) vs. H_2 -air ($\phi=0.28$), $\kappa=140 \text{ s}^{-1}$, numerical simulation using GRI 3.0 mechanism.

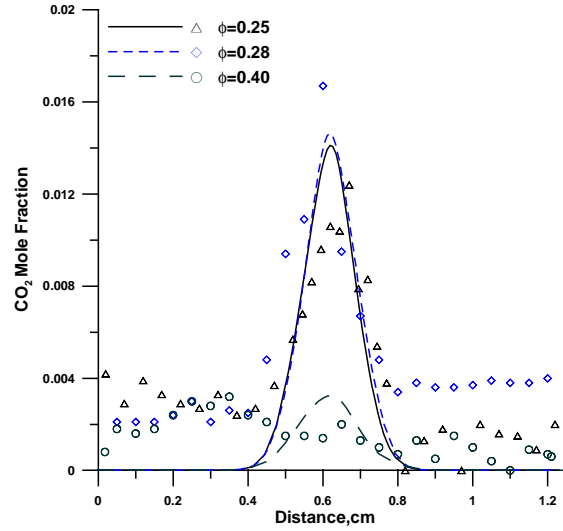


Figure 8. Hot product effect on CO_2 concentration: H_2 -air ($\phi=0.25, 0.28$ or 0.40) vs. CH_4 -air ($\phi=0.54$), $\kappa=140 \text{ s}^{-1}$, numerical simulation using GRI 3.0 mechanism.

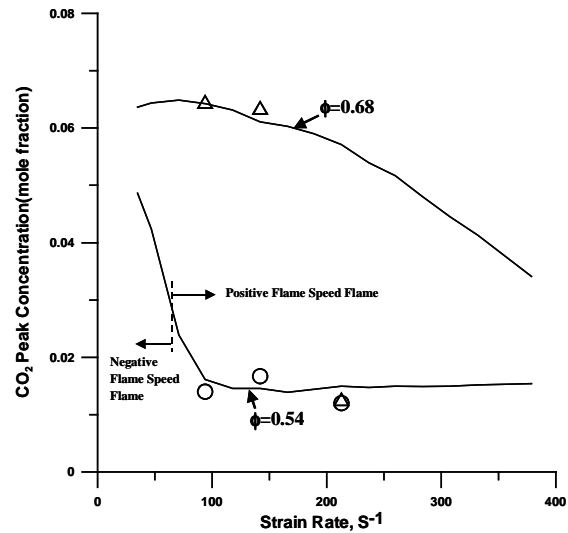


Figure 9. Strain rate effect on CO_2 concentration: CH_4 -air ($\phi=0.54$ or 0.68) vs. H_2 -air ($\phi=0.28$), $\kappa=140 \text{ s}^{-1}$, numerical simulation using GRI 3.0 mechanism.

Figure 9 shows stretch rate effect on peak CO_2 concentration of two series flames: CH_4 -air ($\phi=0.54$ or 0.68) vs. H_2 -air ($\phi=0.28$). The numerical simulations are done using the GRI 3.0 mechanism. Dashed lines approximately indicate transition from self-propagating flames to weak diffusion flames.

(2) C₃H₈ flame versus hot products

Experimental measurements and numerical predictions are also made for propane-air vs. hot products flames. Profiles of temperature and reactant concentrations are compared in Figure 10 for a propane-air ($\phi=0.71$) vs. hydrogen-air ($\phi=0.28$) flame. As seen from the experimental data, a premixed “positive flame speed” flame exists on the side of the stagnation plane for the propane-air mixture. Numerical data is obtained using the M5 mechanism and the optimized propane mechanism by Qin et al. [15]. It is found that experimental profiles of all the major species and temperature match well to the numerically predicted profiles, although the predicted propane flame location is slightly different than the experimental location. For this positive propane flame, two mechanisms seem to predict similar results.

Figure 11 shows a “negative flame speed” propane-air flame. The strain rate is same as the flame shown in Figure 9, but the equivalence ratio is 0.66. This produces a very weak diffusion flame located at the peak of the CO₂ profile. It is obvious that the optimized propane mechanism predicts a stronger flame than the M5 mechanism. It is also noticed that the predicted CO₂ concentration level from M5 mechanism is much lower than the experimental results. This is consistent with previous work [6]. In these low temperature weak diffusion flames, it is interesting that the optimized propane mechanism (429 reactions) gives almost the same results as the experimental results.

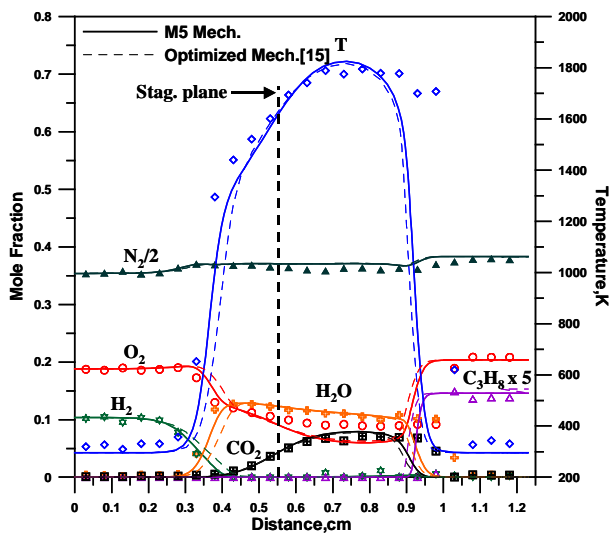


Figure 10. Experimental and numerically-predicted species and temperature profiles for a partially-premixed opposed jet flame: C₃H₈-air ($\phi=0.71$) vs. H₂-air ($\phi=0.28$), $\kappa=140$ s⁻¹.

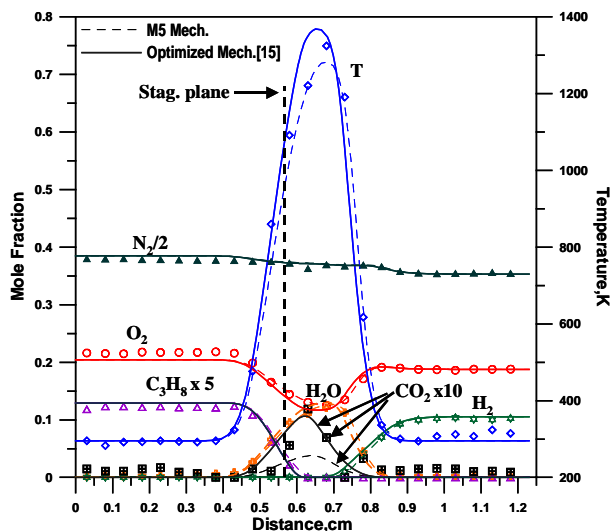


Figure 11. Experimental and numerically-predicted species and temperature profiles for a partially-premixed opposed jet flame: C₃H₈-air ($\phi=0.63$) vs. H₂-air ($\phi=0.28$), $\kappa=140$ s⁻¹.

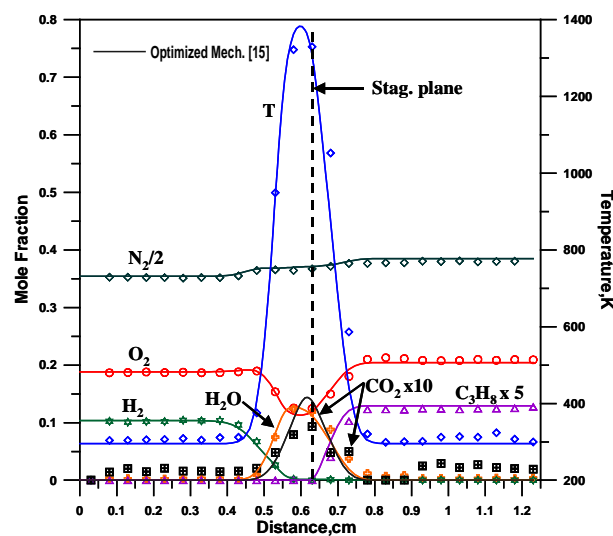


Figure 12. Experimental and numerically-predicted species and temperature profiles for a partially-premixed opposed jet flame: C₃H₈-air ($\phi=0.63$) vs. H₂-air ($\phi=0.28$), $\kappa=252$ s⁻¹.

Figure 12 shows another negative propane-air flame that is near the extinction limit. The predicted results are done using the optimized propane mechanism. All species profiles and temperature profiles have excellent agreement with experimental data. At these conditions, the M5 mechanism predicts an extinction condition and gives no reaction.

CONCLUSIONS

The flame structures of a series of lean partially premixed planar methane- and propane-fueled flames, opposed by hot products produced by lean hydrogen-air flame, are investigated by laser-induced Raman experiments and numerical simulations.

Lean methane-air flames, supported by downstream hot products, show very good agreement between experimental data and numerical results. At high strain rate, the downstream interaction supports a very weak diffusion flame by supplying high temperature products or flame radicals. Among four different chemical kinetic mechanisms, Williams and C2 mechanisms give best temperature profile fit for a self-propagating positive flame speed flame, while all four mechanisms give very similar predictions for a negative flame speed flame.

Experimentally measured partially premixed propane-air flame structures, with downstream hot products support, show good agreement with interaction for self-propagating flame. For negative flame speed propane-air flames, the predicted CO₂ concentration profile with M5 mechanism is still much lower than experimental results, while the optimized propane mechanism gives very good predicted results compared to experimental data.

ACKNOWLEDGEMENTS

The authors would like to acknowledge the U.S. Department of Energy's Office of Basic Energy Sciences who have supported this work through a Partnerships for Academic-Industrial Research (PAIR) grant (No. DE-FG02-98ER14915, with Dr. Alan H. Laufer as the technical monitor).

REFERENCES

1. Jimenez, C., Haworth, D., Poinot, T., Cuenot, B. and Blint, R., (2000), "Numerical Simulations of Combustion in a Lean Stratified Propane-Air Mixture," *Proceedings of Summer Program 2000, Center for Turbulence Research*, pp. 133-144.
2. Sohrab, S. H., Ye, Z. Y., and Law, C. K. (1984), "An Experimental Investigation on Flame Interaction and the Existence of Negative Flame Speeds," *Proceedings of the Combustion Institute* **20**, pp. 1957-1965.
3. Ju, Y., Guo, H., Maruta, K., Niioka, T., (1998), "Flame Bifurcations and Flammable Regions of Radiative Counterflow Premixed Flames with General Lewis Numbers," *Combustion and Flame* **113**, pp. 603-614.
4. Ju, Y., Matsumi, H., Takita, K., and Masuya, G., (1999), "Combined Effects of Radiation, Flame Curvature, and Stretch on the Extinction and Bifurcations of Cylindrical CH₄/Air Premixed Flame," *Combustion and Flame* **116**, pp. 580-592.
5. Tanoff, M. A., and Smooke, M. D., Osborne, R. J., Brown, T. M., Pitz, R. W., (1996), "The Sensitive Structure of Partially Premixed Methane-Air vs. Air Counterflow Flames," *Proceedings of the Combustion Institute* **26**, pp. 1121-1128.
6. Wehrmeyer, J. A., Cheng, Z., Mosbacher, D. M., Pitz, R. W., Osborne, R. J. (2002), "Opposed Jet Flames of Lean or Rich Premixed Propane-Air Reactants versus Hot Products," *Combustion and Flame* **128**, pp. 232-241.
7. Cheng, Z., Wehrmeyer, J. A., and Pitz, R. W. (2002), "Opposed Jet Flames of Lean Premixed Methane-Air Reactants vs. Hot Products," Paper AIAA 2002-4021 presented at 38th AIAA Joint Propulsion Conference, Indianapolis, IN, July 7-10.
8. Kee, R. J., Rupley, F., Miller, J., Coltrin, M., Grcar, J., Meeks, E., Moffat, H., Lutz, A., Dixon-Lewis, G., Smooke, M., Warnatz, J., Evans, G., Larson, R., Mitchell, R., Petzold, L., Reynolds, L., Caracotsios, M., Stewart, W., and Glarborg, P. (1999), *User Manual*, CHEMKIN Collection III.
9. Kim, J. S., Libby, P. A., and Williams F. A. (1992), "On the Displacement Effects of Laminar Flames," *Combustion Science and Technology* **87**, pp. 1-25.
10. Seshadri, K., Puri, I., and Peters, N. (1985), *Combustion and Flame*, **61**, p. 237.
11. Peters, N., (1993), "Flame Calculations with Reduced Mechanisms-An Outline," in *Reduced Kinetic Mechanisms for Applications in Combustion Systems, Lecture Notes in Physics*, N. Peters and B. Rogg (Eds.), Springer-Verlag: Berlin, Vol. M15, Ch. 1, pp 3-12.
12. Smith, G. P., Golden, D. M., Frenklach, M., Moriarty, N. W., Eiteneer, B., Goldenberg, M., Bowman, C. T., Hanson, R. K., Song, S., Gardiner, W. C., Jr., Lissianski, V.V., and Qin, Z. http://www.me.berkeley.edu/gri_mech/
13. <http://maeweb.ucsd.edu/~combustion/cermech/>
14. Haworth, D. C., Blint, R. J., Cuenot, B., and Poinot, T. J. (2000), "Numerical Simulation of Turbulent Propane-Air Combustion with Nonhomogeneous Reactants," *Combustion and Flame* **121**, pp. 395-417.
15. Qin, Z., Lissianski, V., Yang, H., Gardiner, W., Davis, S., and Wang, H., (2000), "Combustion Chemistry of Propane: A Case Study of Detailed Reaction Mechanism Optimization," *Proceedings of the Combustion Institute* **28**, pp. 1663-1669.
16. Darabiha, N., Candel, S. M., and Marble, F. E. (1986), "The Effect of Strain Rate on a Premixed Laminar Flame," *Combustion and Flame* **64**, pp. 203-217.